Applied Numerical Modeling in Geomechanics – 2020 – Billaux, Hazzard, Nelson & Schöpfer (eds.) Paper: 02-06

Viscous Ubiquitous Joints in Comba User-Defined Model for *FLAC3D/3DEC*

C. Detournay[1], G. Meng[2] & P. Cundall[1]
[1] *Itasca Consulting Group, Inc., Minneapolis, MN, USA*
[2] *HydroChina – Itasca R&D Center, Hangzhou, China*

1 INTRODUCTION

Joints or discontinuities in rock mass that are filled with clay material often show a creep behavior. The shear strength of a filled joint is typically less than that of the intact rock. Usually, creep deformation in intact rock is considered negligible compared to creep arising in these joints. Currently, the Comba constitutive model supports logic to represent (up to four) Ubiquitous Joints (Detournay & Cundall, 2014, 2016). It is of interest—for application at the Baihetan site—to supplement the model with viscous behavior in ubiquitous joints (Meng 2016, Meng et al., 2016).

In this project, we consider a creep power law for the ubiquitous joints and we implement it in a numerical scheme that accounts for multiple joints, anisotropic elasticity, as well as plasticity. The model contains two parameters: a coefficient, *A*, and an exponent, *n*, that need to be calibrated using laboratory and/or field experiments.

2 FRAMEWORK

In this work, a creep rate component is added to the Comba ubiquitous joints logic. We consider the power law suggested by Malan et al. (1998) that provides the following relation between steady state creep rate and the stress/strength ratio:

$$\dot{\varepsilon}^{cr} = A\left(\frac{\overline{\tau}}{\overline{\tau}_{\max}}\right)^{n} \tag{1}$$

where τ and $\tau_{\max}$ are the shear stress and maximum shear stress on the joint, respectively, the overbar stands for absolute value, and A and n are calibration parameters that depends on the absolute stress level (as well as the thickness and type of filling).

A local system of axes is defined for the joint; axis 3 is normal to the plane, axis 1 is in the direction of the dip direction vector, and axis 2 is in the direction of the strike. With this convention, the local shear stress on the joint is $\overline{\tau} = \sqrt{\sigma_{13}^2 + \sigma_{23}^2}$, and the shear strength is calculated using Mohr criterion, $\tau_{\max} = c_j - \sigma_{33}\tan\phi_j$ where compressive stresses are negative, c_j is joint friction, and ϕ_j is joint friction.

In the Comba implementation, creep only takes place if the normal stress on the joint, σ_{33}, is compressive (σ_{33} is negative in this case). Also, the law uses a threshold ratio, $s_{\lim}$, above which creep is active (and below which creep does not take place):

$$\frac{\overline{\tau}}{\overline{\tau}_{\max}} > s_{\lim} \tag{2}$$

where, e.g., $s_{\lim} = 30\%$ for unfilled joints, and $s_{\lim} = 10\%$ for filled joints (Glamheden & Hokmark 2010). Finally, the local creep rate components in the joint plane are expressed as follows.

$$\begin{aligned} \dot{\varepsilon}_{13}^{cr} &= \frac{\sigma_{13}}{\overline{\tau}} \dot{\varepsilon}_{cr} \\ \dot{\varepsilon}_{23}^{cr} &= \frac{\sigma_{23}}{\overline{\tau}} \dot{\varepsilon}_{cr} \end{aligned} \tag{3}$$

The elasto-plastic stress-strain behavior is already represented in the Comba model (Detournay et al. 2016). The model incremental stress-strain relations are obtained by superposition of strain contributions from the "intact" rock (column matrix) and from the joints; a creep component acting in the joints is simply added in the formulation.

3 LAW IMPLEMENTATION

The total strain increment is expressed as the sum of elastic, creep, and plastic components. Consistent with the superposition principle, the global stress-strain equations are expressed as follows:

$$\left\{\dot{\sigma}\right\}_G = C_G \left\{\dot{\varepsilon}\right\}_G - C_G \left\{\dot{\varepsilon}^{cr}\right\}_G \Delta t - C_G \left\{\dot{\varepsilon}^{p}\right\}_G \tag{4}$$

where C_G is the global elasticity matrix, the creep component is evaluated as the sum of joint contributions, and Δt is the creep timestep. By convention, we refer to the first, second, and third term in the right hand side of Eq. (4) as elastic guess $\left\{\dot{\sigma}\right\}_G^{guess}$, creep stress correction $\left\{\dot{\sigma}\right\}_G^{cr}$, and plastic stress correction $\left\{\dot{\sigma}\right\}_G^{p}$, respectively. In the Comba formulation, the contribution from joint I to the creep stress correction is evaluated in the local axes of the joint:

$$\left\{\dot{\sigma}\right\}_L^{i,cr} = C_L^i \left\{\dot{\varepsilon}^{cr}\right\}_L^i \Delta t \tag{5}$$

where C_L^i is the elasticity matrix in the local axes of joint i,

$$\left\{\dot{\varepsilon}^{cr}\right\}_L^i = \left\{0,0,0,0,2\dot{\varepsilon}_{13}^{cr},2\dot{\varepsilon}_{23}^{cr}\right\}_L^i \tag{6}$$

and the local creep rate is given by Eq. (3) and (1). The local contribution of joint i is then evaluated in global axes and added to the global contributions of the other joints in the model to provide the total creep stress correction for the step. The creep stress correction is subtracted from the elastic guess before the plastic stress correction is performed using the scheme documented in Detournay & Cundall (2016).

4 ELEMENT TEST

Unconfined visco-elastic element tests under constant vertical pressure *P* are conducted with the Comba model and one active ubiquitous joint. The element is represented in Figure 1. The ubiquitous joint makes an angle θ with the horizontal plane. The local axes are indicated with a prime.

The exact solution for the strain in the local axes is:

$$\varepsilon_{x'z'}^{cr} = A\left(\frac{\sigma_z \sin\theta\cos\theta}{c - \sigma_z \cos^2\theta \tan\phi}\right)^n sign(\sigma_z \sin\theta\cos\theta)t \tag{7}$$

and the global strains are obtained using the following expressions:

$$\begin{aligned}\varepsilon_x &= -2\varepsilon^{cr}_{x'z'}\sin\theta\cos\theta \\ \varepsilon_z &= +2\varepsilon^{cr}_{x'z'}\sin\theta\cos\theta \\ \varepsilon_{xz} &= \varepsilon^{cr}_{x'z'}\left(\cos^2\theta - \sin^2\theta\right)\end{aligned} \tag{8}$$

The creep properties for the simulations are: $A = 0.002$, $n = 4$, and $s_{\lim} = 0$. The joint cohesion is 1, and friction is zero. The displacements obtained at the end of the simulation are shown in Figure 2 for different values of the ubiquitous joint angle (counted positive counter-clockwise from the horizontal plane). A comparison between numerical prediction (red symbol) and analytical value (blue line) of vertical displacement is shown versus creep time on the same plot.

The match between numerical and analytical values of vertical displacement is very good. The displacement vectors are as expected from direct shearing for joint dip angles smaller than 45 degrees. For dip angles larger than 45 degrees, the complementary shearing is exhibited, and for a dip angle of 45 degrees, both direct and complementary shearing modes are represented.

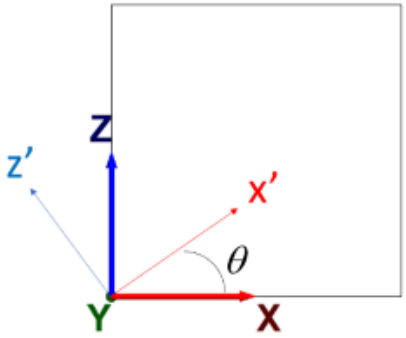

Figure 1. Element and ubiquitous joint representation.

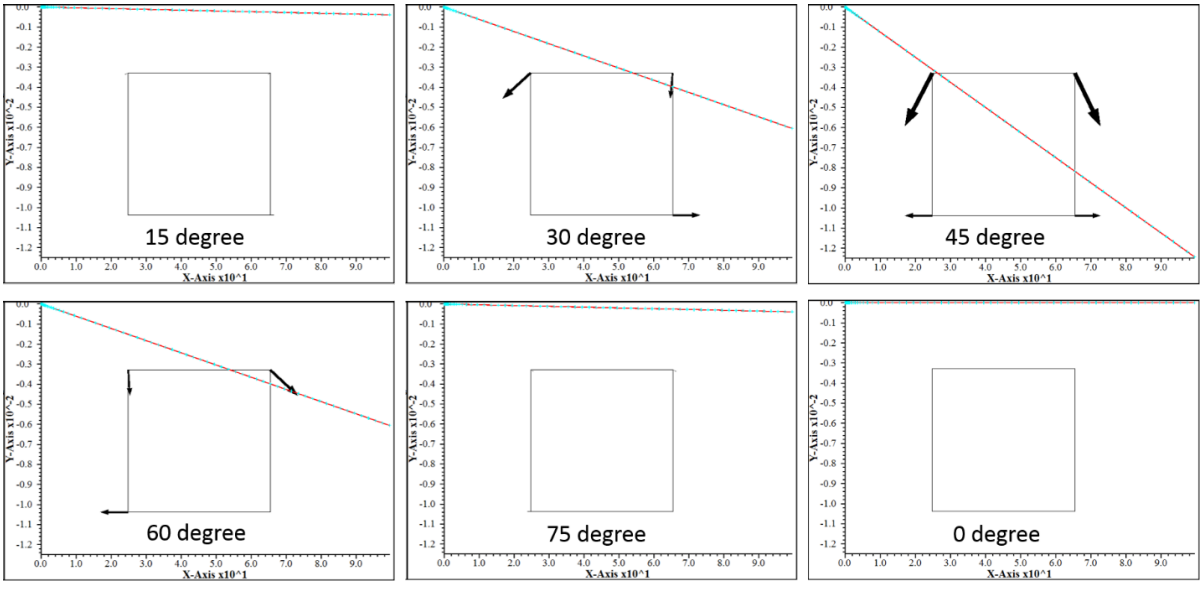

Figure 2. Final displacement vectors for different ubiquitous joint angle, and comparison with exact solution of vertical displacements with creep time.

5 SIMPLE VALLEY PROBLEM

In this example, the two-dimensional mechanical problem of a valley in a three-layer model that is instantaneously filled with water is considered. Three material layers are represented in the model, which is 35 m long and 15 m high. See Figure 3.

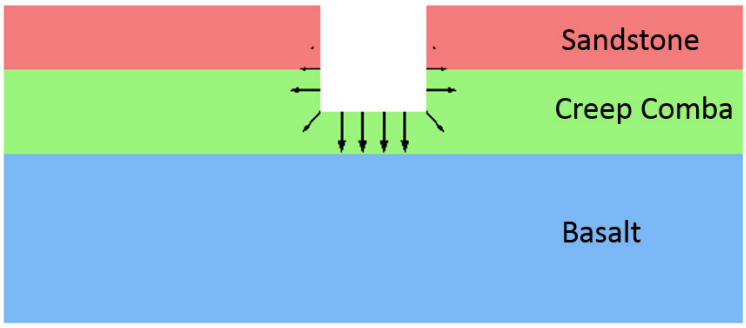

Figure 3. Three-layer model of a valley – applied forces from standing water shown in black.

The numerical modeling includes several steps. First the initial isotropic stress equilibrium for the three horizontal layers is established. Excavation of the valley is simulated. The mechanical pressure from the standing water is applied, and the model is run to equilibrium. Finally, creep can take place in the comba layer and the model is run for a total of 20 time-units. The comba layer has one set of ubiquitous joints. The joint plane makes an angle of θ degrees, counted counter-clockwise with reference to the horizontal. Several inclinations of the ubiquitous joint plane are considered, corresponding to $\theta = 30^o$, 45^o, and 60^o. The simulation results are presented below. Note that there is no plasticity in the model for the comba material properties used in the runs.

The displacements induced by the standing water loading only, and those induced by creep only at the end of the simulation, are shown in Figures 4 to 6.

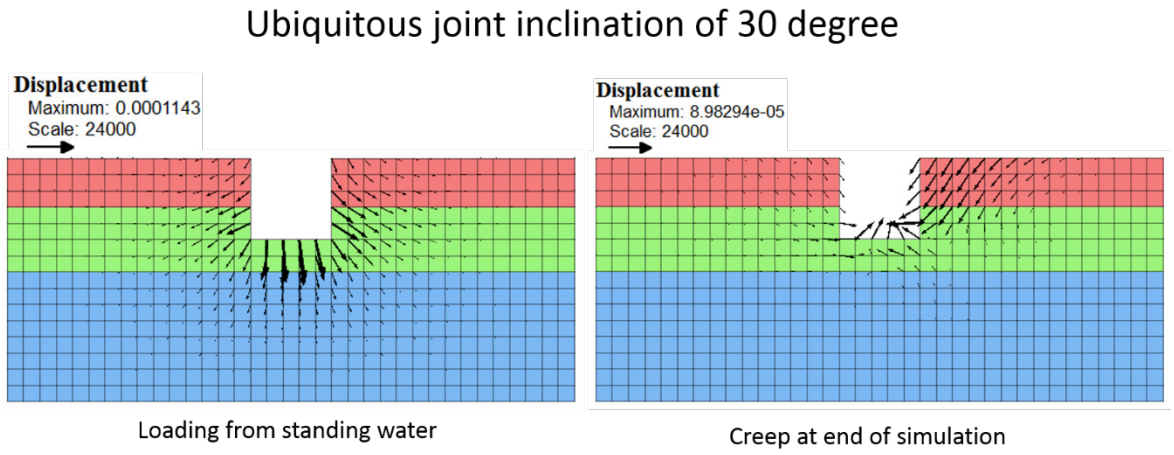

Figure 4. Displacement vectors from static and creep loading at end of simulation case-1.

The displacements from static loading by the standing water (to the left in Fig. 4) are slightly asymmetric. This response is caused by the normal and shear contributions of the joint to the overall elastic stiffness matrix. Although the comba layer is the only one to exhibit a creep behavior, the elastic layers above and below are significantly affected by the creep-induced displacements (right plot in Fig. 4).

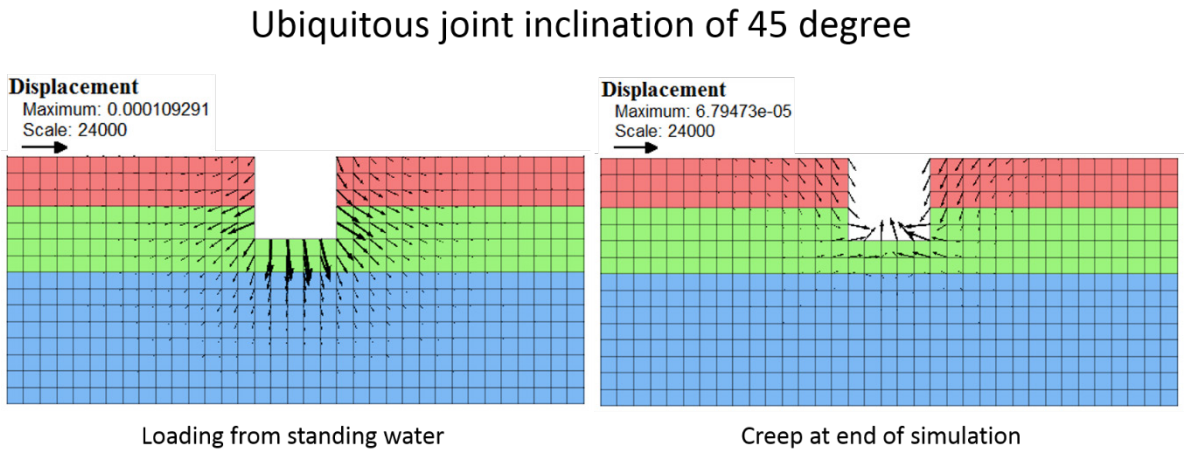

Figure 5. Displacement vectors from static and creep loading at end of simulation case-2.

The creep displacement asymmetry observed to the right in Figure 5 reflects the anisotropic-elastic response of the Comba model in the analyzed cases. When the joint stiffness is much higher than the matrix stiffness, the elastic behavior is governed by the isotropic matrix stiffness, and the observed displacement results are symmetric, as expected.

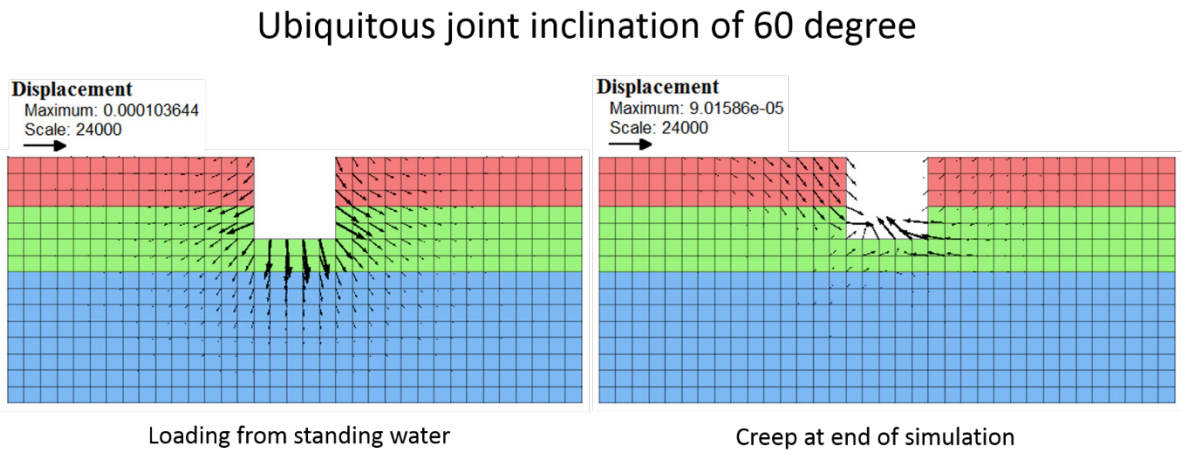

Figure 6. Displacement vectors from static and creep loading at end of simulation case-3.

The overall trend of creep displacements observed on the river banks for the 60 degree case (see Fig. 6) is the reverse of the trend predicted for the 30 degree case (see Fig. 4). These results are consistent with the predictions made in the element case (see Fig. 2): indeed, it appears that the displacement vectors observed in the comba layer are as expected from direct shearing for joint dip angles smaller than 45 degrees. For dip angles larger than 45 degrees, the complementary shearing is exhibited, and for a dip angle of 45 degrees, both direct and complementary shearing modes are represented.

6 CONCLUSIONS

The logic for up to four visco-elasto-plastic joints has been added in the Comba model. Element tests have been conducted for one single joint, and the results compared well to analytic predictions. Also, a simple valley problem has been simulated with the Comba creep model assigned to a layer. The model behavior is reasonable and consistent. However, representative creep parameters for different material joints must be established. Also, more extensive testing remains to be done—with multiple joint sets in both simple and more realistic problems.

REFERENCES

Detournay, C. & Cundall, P.A. 2014. "Comba UDM for *FLAC3D* – Second Progress Report," Itasca Consulting Group, Inc., Report to HydroChina – Itasca R&D, 13-2810. Minneapolis, Minnesota.

Detournay, C. & Cundall, P.A. 2016. "Comba UDM for *FLAC3D* – Matrix Yielding," Itasca Consulting Group, Inc., Report to HydroChina – Itasca R&D, 16-2-4454-01-20TM. Minneapolis, Minnesota.

Detournay, C., Meng, G.T. & Cundall, P.A. 2016. Development of a Constitutive Model for Columnar Basalt. In: *Proceedings of the 4th Itasca Symposium on Applied Numerical Modeling, Lima, Peru, 7-9 March 2016*. Minneapolis: Itasca.

Glamheden, R. & Hokmark, H. 2010. Creep in jointed rock masses – State of knowledge. Svenk Karnbranslehantering AB, Swedish Nuclear Fuel and Waste Management Co. ISSN 1402-3091, SKB R-06-94. www.skb.se

Itasca Consulting Group, Inc. 2017. *FLAC3D — Fast Lagrangian Analysis of Continua in Three Dimensions*, *Ver. 6.0.* Minneapolis: Itasca.

Malan, D.F., Drescher, K. &Vogler, U.W. 1998. Shear creep of discontinuities in hard rock surrounding deep excavations. In: Rossmanith H-P (ed). *Proceedings of the Third International Conference on Mechanics of Jointed and Faulted Rock – MJFR-3, Vienna, Austria, 6-9 April 1998*. Rotterdam: Balkema, pp473-478.

Meng, G.T. 2016. DEM approach for anisotropic behavior analysis of columnar jointed basalt. In: *Proceedings of the 4th Itasca Symposium on Applied Numerical Modeling, Lima, Peru, 7-9 March 2016*. Minneapolis: Itasca.

Meng, G.T., Detournay, C. & Cundall, P.A. 2016. Continuum/discrete numerical simulation of columnar basalt in large-scale underground excavations. In: *50th U.S. Rock Mechanics/Geomechanics Symposium (Houston, Texas, June 2016)*. ARMA 16-211. Alexandria: ARMA.